Biomaterials Science

Printed Nanofilms Mechanically Conforming to Living Bodies

Journal:	*Biomaterials Science*
Manuscript ID	BM-MRV-10-2018-001290.R1
Article Type:	Minireview
Date Submitted by the Author:	12-Dec-2018
Complete List of Authors:	Yamagishi, Kento; Waseda University, Research Organization for Nano & Life Innovation Takeoka, Shinji; Waseda University, Faculty of Science and Engineering Fujie, Toshinori; Waseda University, Waseda Institute for Advanced Study; JST, PRESTO; Tokyo Institute of Technology, School of Life Science and Technology

Manuscript for Biomaterials Science (Minireview)

Printed Nanofilms Mechanically Conforming to Living Bodies

*Kento Yamagishi[1], Shinji Takeoka[2], Toshinori Fujie[3,4,5]**

[1]Research Organization for Nano & Life Innovation, Waseda University, Tokyo 162-8480, Japan.

[2]Faculty of Science and Engineering, Waseda University, Tokyo 162-8480, Japan.

[3]Waseda Institute for Advanced Study, Waseda University, Tokyo 162-8480, Japan.

[4]JST PRESTO, Saitama 332-0012, Japan.

[5]School of Life Science and Technology, Tokyo Institute of Technology, Yokohama 226-8501, Japan.

* Corresponding author at: Waseda Institute for Advanced Study (WIAS), Waseda University, 2-2 Wakamatsu-cho, Shinjuku-ku, Tokyo 162-8480, Japan. Tel: +813-5369-7324, Fax: +813-5369-7324
E-mail address: t.fujie@aoni.waseda.jp (T. Fujie)

Present address: School of Life Science and Technology, Tokyo Institute of Technology, B-50, 4259 Nagatsuta-cho, Midori-ku, Yokohama 226-8501, Japan. Tel&Fax: +81-45-924-5712, E-mail: t_fujie@bio.titech.ac.jp (T. Fujie)

Abstract

It is anticipated that flexible wearable/implantable devices for biomedical applications will be established for the development of medical diagnostics and therapeutics. However, these devices need to be compatible with the physical and mechanical properties of the living body. In this minireview, we introduce free-standing polymer ultra-thin films (referred to as "polymer nanosheets"), for which a variety of polymers can be selected as building blocks (*e.g.*, biodegradable polymers, conductive polymers, and elastomers), as a platform for flexible biomedical devices that are mechanically compatible with the living body, and then we demonstrate the use of "printed nanofilms" by combining nanosheets and printing technologies with a variety of inks represented by drugs, conductive nanomaterials, chemical dyes, bio-mimetic polymers, and cells. Owing to the low flexural rigidity ($< 10^{-2}$ nN m) of the polymer nanosheets, which is within the range of living brain slices (per unit width), the flexible printed nanofilms realize bio-integrated structure and display various functions with unique inks that continually monitor or direct biological activities, such as performing surface electromyography, measuring epidermal strain, imaging tissue temperature, organizing cells, and treating lesions in wounds and tumors.

1. Introduction

To advance diagnostics and therapeutics using bio-interfacing medical devices, it is critically important to resolve the mechanical mismatch between electronic medical devices and the living human body. Despite the rapid development of flexible and stretchable skin-contact devices for bio-monitoring[1] such as electromyography (EMG)/electrocardiography (ECG) sensors[2,3,4,5,6,7] and epidermal strain gauges[2,3,8,9,10,11], those devices face several drawbacks related to the lack of adhesiveness to the skin due to limitations to the thickness and softness of electronic parts. This results in the need for intermediate adhesives, which constrain the skin and interfere with the natural movements of the body. In addition, demands for wireless communication technology have grown, not only for wearable but also for implantable devices, to avoid the burden of payload with batteries and connective lead wires on the wearers/patients, including animals and humans. In this regard, implantable devices have become miniaturized and battery-free, resulting in a reduction in the mechanical incompatibility with the living body[12,13,14]. However, those devices have been fixed or implanted by surgical suture or with the aid of medical glue to attach them to structurally uneven or wet living tissue surfaces even in relatively stable positions in the body, such as to the skull or spinal cord, which results in local strong tension to the tissue and causes inflammation of the tissue or undesirable adhesion of the tissues surrounding the device. Therefore, it is critically important to focus on the mechanical properties of the platform of wearable/implantable devices as well as those of biological tissues including skin, muscle and tumor tissues for the design and construction of mechanically bio-conformable devices.

In this minireview, with the aim of facilitating the development of tailor-made biomedical devices that mechanically conform to the living body, including biological tissues and organs, we focus on free-standing polymer ultra-thin films (referred to as “polymer nanosheets”[15]) with a thickness of less than 1 μm as a platform for ultra-flexible devices.

Then, taking advantage of several printing technologies, as exemplified by gravure printing[16], inkjet printing[17,18], microcontact printing[19,20], and chemical modification[21,22], we describe the development of "printed nanofilms" by combining nanosheets and a variety of unique inks represented by conductive nanomaterials[16,17,18,23], chemical dyes[24], bio-mimetic adhesives[22], drugs[25,26,27], and cells[19,20,28,29] (**Fig. 1**). The printed nanofilms can provide a range of functions and biomedical applications on/in the living body: integrating electronic devices[18,22], chemicals[24,26], and cells[29] on/in the living body; monitoring biological information (e.g., surface electromyograms[16], brain neuronal signals[30], tissue temperature[24] and extracellular pH[31]); and clinically treating inflammatory sites like wounds[26] and tumors[22]. In the text below, we review the principle of the polymer nanosheets including their mechanical and adhesive properties, followed by the definition, fabrication, and applications of printed nanofilms constructed based on ultra-conformable polymer nanosheets and several printing technologies.

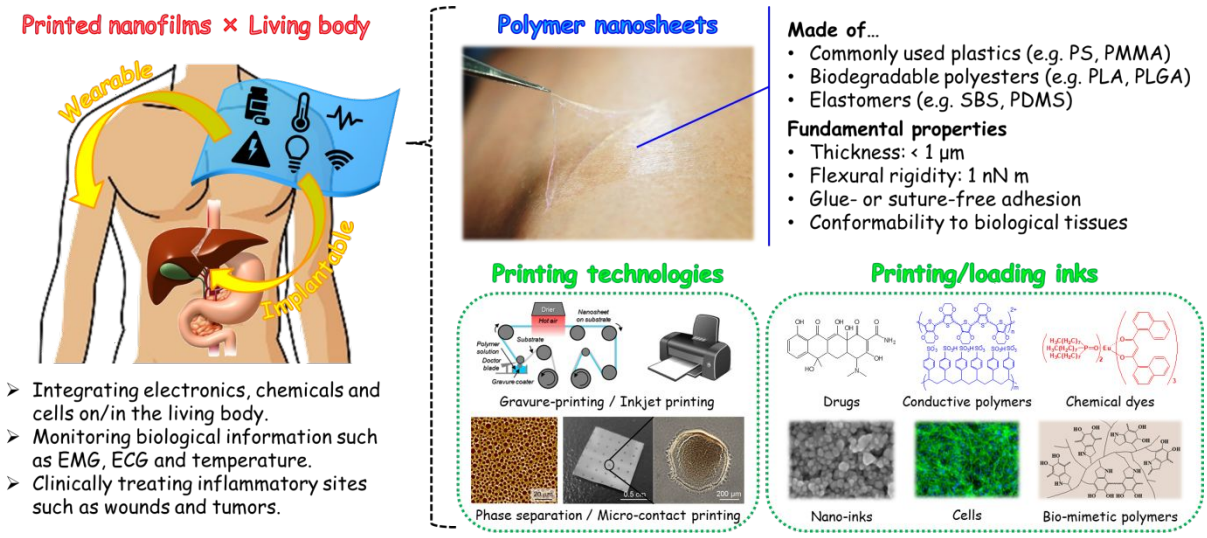

Fig. 1 Schematic illustration of printed nanofilms conforming to the living body. Integration of printing technologies using various inks to ultra-conformable polymer nanosheets for the development of printed nanofilms as wearable/implantable sheet devices in biomedical applications. Images are partially reproduced from ref. 15, 19, 22, 28, and 29.

2. Ultra-flexible and ultra-conformable polymer nanosheets

As shown in **Fig. 2A**, most of the materials constituting electrical devices have a higher Young's modulus (> 100 kPa)[32] than biological tissues such as heart (20–500 kPa[33]) and brain (0.1–16 kPa[34,35]). There have been several studies demonstrating that the encapsulation of miniaturized devices in soft materials, as exemplified by polydimethylsiloxane (PDMS) or Ecoflex®, reconciled the mechanical mismatch between hard electronic elements and soft biological tissues and minimized the mechanical interference with animal/human behavior[13,14,36]. In addition, the mechanical conformability of a film material is known to be correlated to its flexural rigidity[37], *D*, defined by the following equation:

$$D = \frac{Et^3}{12(1-\nu^2)}$$

where *E*, *t*, and *v* represent Young's modulus, thickness, and Poisson's ratio of the film, respectively[38]. As the flexural rigidity *D* is proportional to the cube of the thickness *t*, reducing the thickness is the most effective approach to decreasing flexural rigidity (**Fig. 2B**). While there is a limit to the thickness of electrical components, materials for a platform that seals the entire device can be thinner and softer. Therefore, the development of ultrathin films with low flexural rigidity is critically important to solve the mechanical mismatch between electrical devices and the living body and to provide more conformable adhesion to the surfaces of biological tissues.

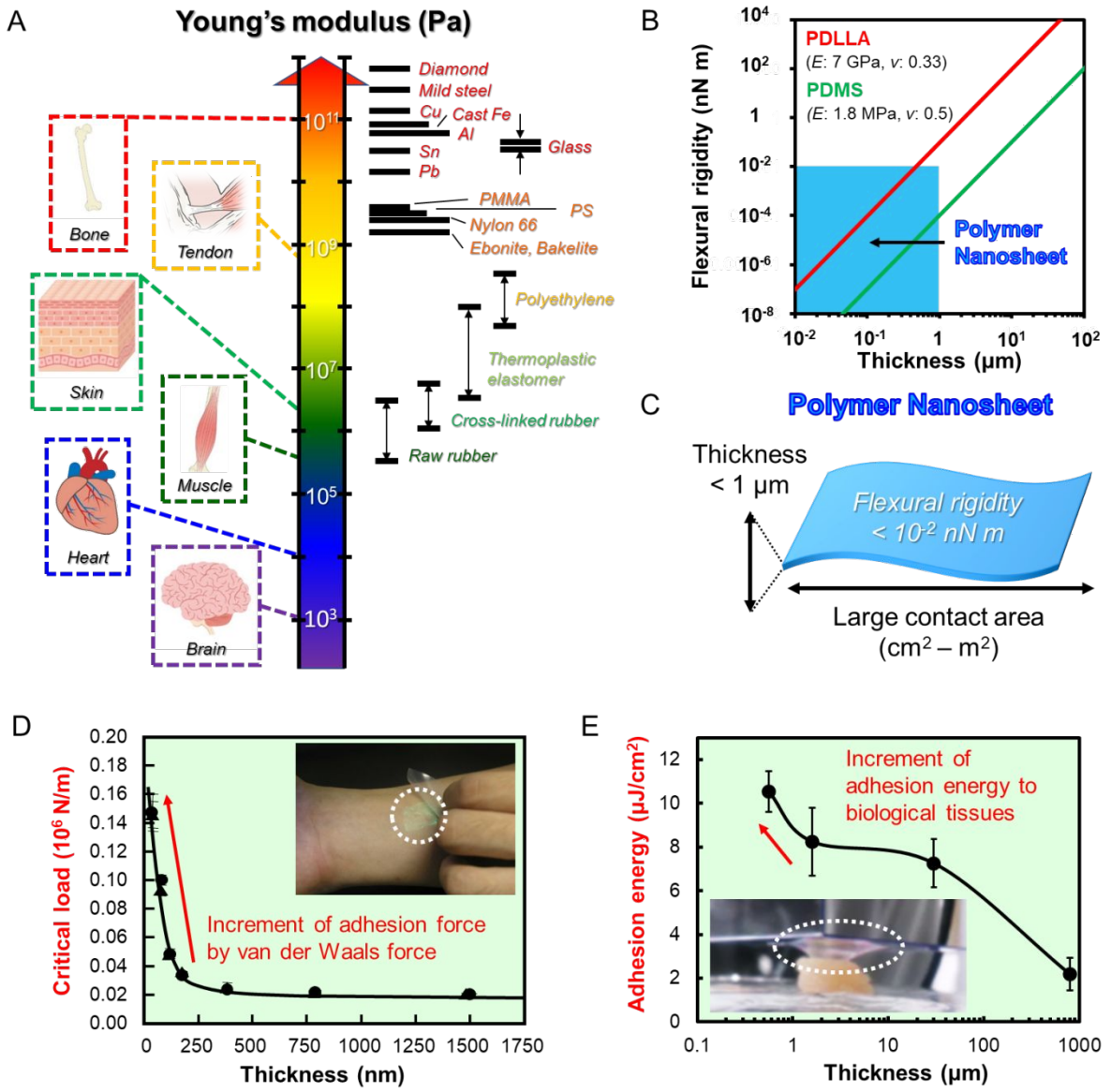

Fig. 2 Ultra-flexible and ultra-conformable polymer nanosheets. (A) Young's moduli of biological tissues and materials[32]. (B) Theoretical relationship between thickness and flexural rigidity of poly(L-lactic acid) (PLLA) and PDMS, where the Young's moduli E and Poisson's ratios v of the polymers are set as follows: E_{PLLA}: 7 GPa, v_{PLLA}: 0.33[39,40], E_{PDMS}: 1.8 MPa[41], and v_{PDMS}: 0.5[42]. The range of each line crossing the light blue area represents the range of polymer nanosheets' values (thickness: < 1 μm, flexural rigidity: < 10^{-2} nN m). (C) Schematic illustration of a free-standing polymer nanosheet. (D) Adhesiveness of polysaccharide nanosheets evaluated by a micro-scratch test. Inset: image of a polysaccharide nanosheet adhered to the skin. The data are partially reproduced from ref. 25. (E) Tissue adhesiveness of

PDMS nanosheets evaluated by a tack separation test. Inset: Image of a PDMS nanosheet adhered to chicken muscle during a tack separation test. The data are partially reproduced from ref. 22.

Free-standing polymer nanosheets with flexural rigidity of less than 10^{-2} nN m (**Fig. 2C**), which is the same range as that of living brain slice tissue per unit width (10^{-4}-10^{-1} nN m)[34], generate unique physical properties, including flexibility, van der Waals force-based physical adhesion, and surface conformability[15]. We demonstrated the fabrication of free-standing polymer nanosheets by a laboratory-scale process like spin-coating and layer-by-layer techniques, as well as an industrially applicable roll-to-roll process based on gravure printing on several solid substrates, e.g. silicon wafer, glass, and plastic. There are two major strategies for obtaining free-standing polymer nanosheets from those temporary substrates: "sacrificial" and "supporting" layer methods[43]. The nanosheet can be made of a variety of polymers, including commonly used plastics like polystyrene (PS) and polymethyl methacrylate (PMMA)[24]; biodegradable polyesters like polysaccharides[44], polylactic acid (PLA)[39], and poly(lactic-co-glycolic acid) (PLGA)[19]; and elastomers like polystyrene–polybutadiene–polystyrene (SBS) triblock copolymer[45] and PDMS[22].

The mechanical properties of "plastic" nanosheets made of PS[45] and PLLA[39] were evaluated by an air bulge test[46] to obtain their elastic moduli or strain-induced buckling instability for mechanical measurements (SIEBIMM)[40,47] to obtain their Young's moduli because these nanosheets are too thin and fragile to be applied to the standard set-up of a tensile test. In contrast, "elastomer" nanosheets made of SBS[45] and PDMS[22] were evaluated by the tensile test to obtain their Young's moduli. As shown in **Table 1**, the mechanical properties of the polymer nanosheets are strongly dependent on the glass transition temperature (T_g) of the polymer; the variation of T_g determines the elastic/Young's moduli of the prepared nanosheets in the range from MPa to GPa. With their ultrathin thickness (< 1

μm), the nanosheets show flexural rigidity of < 10^{-2} nN m. Interestingly, as the flexural rigidity is also proportional to the elastic/Young's moduli, elastomer nanosheets with a thickness of several hundreds of nanometers have a range of flexural rigidity (10^{-6} to 10^{-4} nN m) similar to that of plastic nanosheets with a thickness of several tens of nanometers. This indicates that elastomers having a ~1000-fold lower Young's modulus (1~10 MPa) than plastics (> 1 GPa) can exhibit the unique properties of polymer nanosheets (D < 10^{-2} nN m) even if their thickness is 10-fold larger than that of plastic nanosheets, which is in accordance to the equation of flexural rigidity.

Table 1 Mechanical properties of polymer nanosheets. For PS and PLLA nanosheets, the flexural rigidity was calculated using their elastic modulus obtained by an air bulge test and, for SBS and PDMS nanosheets, using their Young's modulus obtained by a tensile test. The data are partially reproduced from ref. 22, 39, and 45.

Polymer	T_g (°C)	Thickness (nm)	Elastic/Young's modulus (GPa)	Flexural rigidity (nN m)
PS	100	127 ± 10	0.9 ± 0.05	1.7×10^{-4}
		217 ± 5	1.2 ± 0.33	1.1×10^{-3}
PLLA	58	23 ± 5	1.7 ± 0.1	1.9×10^{-6}
		60 ± 14	3.1 ± 0.5	6.3×10^{-5}
SBS	-70	212 ± 16	0.0057 ± 0.0012 (5.7 ± 1.2 MPa)	5.1×10^{-6}
		690 ± 79	0.0049 ± 0.0008 (4.9 ± 0.8 MPa)	1.5×10^{-4}
PDMS	-125	561 ± 87	0.00076 ± 0.00013 (0.76 ± 0.13 MPa)	1.5×10^{-5}

As the surface of the living biological tissues is not flat but rough, the conformability, *i.e.*, the surface followability of thin-film materials, that can be obtained by reducing their flexural rigidity[37], should be improved to increase the contact area between tissue and film. With the low flexural rigidity (< 10^{-2} nN m), the polymer nanosheets allows for ultra-conformable glue-free adhesion to various surfaces via van der Waals interaction. The adhesive properties of polymer nanosheets were investigated using a micro-scratch test

by which the critical loading force required to scratch a nanosheet off a substrate was measured[48]. As shown in **Fig. 2D**, it was found that the adhesive strength of polysaccharide nanosheets to an SiO_2 substrate dramatically increased as the thickness decreased below 200 nm[25]. This characteristic of the nanosheets allows for physical adhesion onto various substrates, including human skin, without the use of adhesives or surface functionalization. Moreover, we evaluated the tissue-adhesive properties of elastomer nanosheets by a tack separation test[22]. As shown in **Fig. 2E**, dependence of the adhesion energy on the thickness was clearly observed in PDMS nanosheets. The adhesion energy of the 560-nm-thick PDMS nanosheet to the chicken muscle was five times higher than that of the 800-μm-thick PDMS bulk film. Interestingly, the PDMS nanosheets showed the drastic increase of the adhesive strength at thicknesses below 1 μm, while polysaccharide nanosheets exhibited this phenomenon below a few hundred nanometers. This result is derived from the lower Young's modulus of the PDMS than that of polysaccharides. The micro-scratch test and tack separation test for the evaluation of the adhesive properties of the plastic and elastomeric nanosheets clearly shows that the adhesion strength of the polymer nanosheets dramatically increases when their flexural rigidity is less than 10^{-2} nN m, *i.e.*, the thickness of plastic and elastomeric nanosheets is less than hundreds of nm and a few μm, respectively. Therefore, the adhesive property of polymer nanosheets is strongly attributed to their thickness, and at the same time, the flexural rigidity which provides conformable adhesion to the target surface with a large contact area[49].

3. Printed nanofilms for biomedical applications

3.1. Printed nanofilms: integration of printing technologies to polymer nanosheets

The progress of printing technologies has enabled "three-dimensional (3D) bioprinting", of which concept is the integration of cells into the conventional 3D printing technologies including inkjet, micro-extrusion, and laser-assisted printing techniques, that greatly

contributed to the 3D fabrication of complex tissue structures for biomedical applications in the field of tissue engineering and regenerative medicine[50,51]. More recently emerged "4D bioprinting" is a technique to print external stimuli-responsive biomaterials to construct dynamic 3D biological tissues that are capable of shape transformation[52,53]. In addition, the rapid progress of printed electronics, *i.e.*, technologies for printing conductive inks, has provided a wide range of all-printed biodevices including bioelectrodes for EMG recording[54] as well as electrochemical sensors for glucose[55] and DNA[56]. As described in the previous sections, polymer nanosheets, made of a variety of polymers, have unique and adaptable physical properties that would be compatible with those of the living body as a platform of flexible biomedical devices. Therefore, with combined technologies of printed electronics and 3D/4D bioprinting, various functions can be integrated on/in the structure of the polymer nanosheets and thus we may further augment their potential applicability.

In this section, "printing technologies" represent surface coating/modification techniques including gravure-printing (including industrial-scale roll-to-roll process)[16], polymer brush coating[21], and mussel-inspired polydopamine coating[57,22] as well as patterning techniques including drop-on-demand inkjet printing[18,17], phase separation-based patterning[28,29], and micro-contact printing[19]. In contrast, "printing/loading inks" cover a wide range of materials including drugs, chemical dyes, conductive polymers, blend polymers, nanoparticles and cells. With this concept, we developed "printed nanofilms" with unique functions embodied on living tissues and organs by combining polymer nanosheets and printing technologies using a variety of inks. Herein, we review some examples of applications of printed nanofilms as mechanically compatible biomedical materials/devices for the living body. **Table 2** summarizes the classification and description of printed nanofilms in terms of application.

Table 2 Classification and description of printed nanofilms in terms of application.

Category	Building block of nanosheet	Printing technologies	Printing/loading inks	Application	Main finding	References
Wearable devices	PDLLA	Gravure-printing	PEDOT:PSS	Surface EMG recording	The PEDOT:PSS/PDLLA conductive nanosheets showed as high a signal-to-noise ratio as clinically approved standard pre-gelled Ag/AgCl electrodes.	16
	SBS	Gravure-printing Inkjet-printing	PEDOT:PSS	Epidermal strain sensor	The SBS nanosheet minimized the obstruction of the skin's natural deformations and the ultrathin epidermal strain sensor measured the skin strain (~2%) on a forearm caused by the extension of the wrist joint.	17
	SBS	Gravure-printing Inkjet-printing	AgNP	Ultra-conformable electronics	With the soldering-free process, electronic elements were physically and electrically fixed on the conductive lines, resulting in the operation of the nanosheet electronics on the human skin.	18
Bioimaging	PMMA PS	Spin-coating	EuDT Rhodamine 800	Nanosheet thermometer	The ratiometric thermometry with the nanosheet thermometer demonstrated mapping and visualization of temperature shift of the living tissue derived from muscular activity in an insect.	24
	PDLLA PAH PAA	Spin-coating Chemical conjugation	Fluorescein Nile red	pH sensing nanosheet	The pH sensing nanosheet enabled the ratiometric imaging of pH changes in a leaf, namely the apoplastic ion milieu responding to an external NaCl stress.	31
Tissue engineering	PDLLA	Gravure-printing Phase separation	C2C12 cells	Cellular scaffold	The PDLLA porous nanosheet played a key role for engineering hierarchical organization of the constituent cells by contributing to the interconnection between adjacent cell layers.	28
	PDLLA	Gravure-printing Phase separation	ASCs	Wound healing	The trilayered ASCs-laden porous nanosheet achieved the in situ homogeneous transplantation of ASCs onto a dorsal skin defect model in diabetic mice and contributed to wound healing.	29
	PLGA	Spin-coating Micro-contact printing	RPE-J cells	Local delivery of cell sheets	The micropatterned nanosheets consisting of biodegradable PLGA demonstrated local delivery of RPE cells for the treatment of Age-related macular degeneration (AMD).	19
Implantable devices	PDMS	Gravure-printing	PDA	Implantable and wireless PDT	The PDA-PDMS nanosheet-based tissue-adhesive optoelectronic device was stably fixed on the tissue surface and demonstrated the local antitumor effect for tumors through metronomic PDT.	22

PDLLA: poly(D,L-lactic acid), PEDOT:PSS: poly(3,4-ethylenedioxythiophene):poly(styrenesulfonate), EMG: electromyography, SBS: polystyrene–polybutadiene–polystyrene, AgNP: silver nanoparticle, PMMA: polymethyl methacrylate, PS: polystyrene, EuDT: Eu-tris (dinaphthoylmethane)-bis-trioctylphosphine oxide, PAH: poly(allylamine hydrochloride), PAA: poly(acrylic acid), ASCs: adipose-tissue derived stem cells, PLGA: poly(lactic-co-glycolic acid), RPE: retinal pigment epithelial, PDMS: polydimethylsiloxane, PDA: polydopamine, PDT: photodynamic therapy.

3.2. Gravure-printed conductive nanosheets for ultra-conformable bioelectrodes

The introduction of electrical conductivity into the polymer nanosheets would enable the development of ultra-conformable skin-contact electronics with higher flexibility and adhesion, while also being less noticeable to the user, than conventional wearable devices. Moreover, the extension of the processing technologies of flexible thin-film devices to scalable industrial fabrication is essential for real-world applications. Towards this aim, we focused on one of the most widely used conductive polymers, poly(3,4-ethylenedioxythiophene):poly(styrenesulfonate) (PEDOT:PSS)[23,16]. Conductive nanosheets were fabricated by a roll-to-roll gravure-printing of PEDOT:PSS aqueous dispersion on a mechanically supporting nanosheet made of PLA or SBS. As a demonstration of skin-contact applications, the PEDOT:PSS/PLA conductive nanosheets were tested as skin-contact bioelectrodes for the measurement of surface EMG (sEMG) for monitoring bioelectrical signals (**Fig. 3A**)[16]. The results showed that these unperceivable nanosheet electrodes successfully recorded the stepwise increase of sEMG signal depending on the

increment of the pressure applied by a subject's hand grasping a pressure gauge. Notably, the conductive nanosheets showed as high a signal-to-noise ratio (SNR = 36.9 dB) as clinically approved standard pre-gelled Ag/AgCl electrodes (SNR = 35.7 dB)[16]. This demonstration opens up the possibility of using this approach not only in healthcare applications but also in other practical or medical fields, such as prosthetics, wearable robotics, and sports science. Moreover, direct patterning of PEDOT:PSS on polymer nanosheets using other printing technologies like inkjet printing[58,59,60,61,62,63], screen printing[64,65,66], and spray coating[67,68,69] should provide ultra-conformable multi-electrodes for more precise motion analysis of humans.

3.3. Inkjet-printed nanosheet electronics for skin-contact devices

The convenient fabrication of electrical circuits on film substrates is important for the development and expansion of smart printed flexible electronics[70]. In the rapid progress of printing technologies on flexible sheet-type substrates, there have been emerged ultra-thin film or tattoo based conformable printed electronic devices such as capacitors[71,72], transistors[73,74,75] and photovoltaics[76,77]. For the development of printed nanofilms that can detect or monitor the bioelectrical information such as EMG, ECG and neuronal signals, the direct printing of conductive inks is an essential technology. While gravure-printing enables the scalable fabrication of homogeneous conductive polymer nanosheets, the patterning of conductive materials on polymer nanosheets is also required for the development of printed nanofilms with more complex circuits. Hence, we focus on the drop-on-demand inkjet printing of conductive inks, as exemplified by conductive polymers, metal nanoparticles and carbon nanomaterials, on the polymer nanosheet.

As one demonstration of the inkjet-printed nanofilms, we developed an ultrathin epidermal strain sensor constructed with PEDOT:PSS conductive patterns on an SBS nanosheet.[17] The ultrathin structure and glue-free conformable adhesion of the SBS nanosheet

(around 320 nm thick) minimized the obstruction of the skin's natural deformations. With the ultrathin epidermal strain sensor, we successfully measured the skin strain (~2%) on a forearm caused by the extension of the wrist joint (**Fig. 3B**). The printed nanofilm-based ultra-conformable epidermal strain sensor should thus be a powerful tool for precise detection of the motion of the living body, as well as in soft robots.

In addition, we also demonstrated direct inkjet printing of Ag nanoparticles (AgNP) on the SBS nanosheet without dewetting and/or agglomerates by coating an ink-absorbing layer (acrylic-copolymer) on the top of the nanosheet to increase its surface wettability as well as water-absorption. Taking advantage of the van der Waals force-based physical adhesion of the SBS nanosheet, we achieved the soldering-free fixation of small electronic elements. As a demonstration, chip LEDs were sandwiched between two layers of elastomeric SBS nanosheets (each layer: ~380 nm thick), on one of which AgNP-based conductive lines (~720 nm thick) were inkjet-printed[18]. With this soldering-free process, electronic elements were physically and electrically fixed on the conductive lines, resulting in the operation of the nanosheet electronics on the human skin (**Fig. 3C**). The technique of coating of the ink-absorbing layer on the surface of the polymer nanosheets will be useful for manufacturing a variety of printed circuits regardless of the component of polymer nanosheets.

3.4. Chemical dye-loaded nanosheet sensors for mapping biological activity

The loading of environmentally-responsive chemical dyes including indicators of temperature, pH, and specific ions into the polymer nanosheets produces ultra-thin chemical sensors that enable the monitoring of the biological conditions in organs, tissues, and cells. In particular, to locate sites of thermogenesis in the living biological tissues, global mapping of temperature is a more effective method than spot thermometry. Hence, we developed thermosensitive luminescent dye-embedded polymer nanosheets. With the "nanosheet

thermometer", we demonstrated mapping and visualization of temperature shift of the living tissue derived from muscular activity in an insect (**Fig. 3D**)[24]. A key technology of the constructed sensor is "ratiometric" thermometry, which can eliminate the undesired shift in luminescence intensity due to the focal drift or z-axis displacement of the insect by calculating the ratio of the intensities of two different dyes; thermosensitive (Eu-tris (dinaphthoylmethane)-bis-trioctylphosphine oxide: EuDT) and insensitive (Rhodamine 800) dyes. To avoid the possible risk of interaction between the two dyes, we loaded each dye in different nanosheet and those two nanosheets were stacked together with the physically adhesive property of the nanosheets. The high transparency of the nanosheets did not interfere with the obtained fluorescent values of both dyes and provided an accurate ratiometric measurement of the temperature distributions. The printed nanofilm-based microthermography is a promising technology to microscopically explore the heat production/transfer in living cells, tissues and organs with higher spatial resolution than conventional thermometric technologies as typified by infrared thermography. Moreover, the integration of conventional fully-printable electrochemical sensors for other factors such as pH, ions and glucose[78] into the nanosheet should enable the creation of ultra-conformable multi-sensing devices for detecting biological information from the living body.

3.5. Phase separation-based porous nanosheets as cellular scaffolds for tissue engineering

Cellular scaffold materials for tissue engineering should have biocompatibility, biodegradability and a porous structure for loading cells. Taking advantage of the phase separation of blended polymers, one of the simple patterning techniques to obtain the porous structure, we developed a porous nanosheet as a flexible, permeable and biodegradable cellular scaffold. By gravure-printing a polymer blend solution of poly(D,L-lactic acid) (PDLLA)/PS, phase separation occurred in the nanosheet as a result of the immiscibility of

the blended polymers. Immersing the nanosheet in cyclohexane allowed for the selective dissolution of island regions of PS, followed by the generation of a PDLLA nanosheet with a microporous structure (thickness: ~150 nm, mean pore size: ~4 μm, flexural rigidity: $< 10^{-2}$ nN m according to **Fig. 2B**). We demonstrated that the biodegradable PDLLA porous nanosheet played a key role for engineering hierarchical organization of the constituent cells by contributing to the interconnection between adjacent cell layers via the porous nanosheet with secreted extracellular proteins. Moreover, a rolled construct of the porous nanosheet provided a spontaneous formation of the anisotropic alignment of muscle cells, replicating circular muscle in the intestinal wall or the tunica media in an arterial wall (**Fig. 3E**)[28].

As another application of cell-laden porous nanosheets, we developed an engineered scaffold for a local, homogeneous and rapid transplantation of proliferating stem cells as a promising early-phase treatment method for deep burn injuries and intractable ulcers. The porous nanosheets (around 150 nm thick) with a porous structure (mean pore diameter: 4 μm) allowed the proliferation of adipose-tissue derived stem cells (ASCs) and provided sufficient nutrient inflow between cellular layers. With a trilayered ASCs-laden porous nanosheet, we achieved the *in situ* homogeneous transplantation of ASCs onto a dorsal skin defect model in diabetic mice and contributed to wound healing (**Fig. 3F**)[29]. The porous nanosheets are expected to contribute to a better understanding of integrated cellular systems, and ultimately toward the development of a cell therapy for wound healing or regenerative medicine.

As a technology to generate micro-patterns of cells, we also demonstrated inkjet and microcontact printing of cell-adhesive proteins such as fibronectin on the polymer nanosheet to align C2C12 skeletal myoblasts, which enhanced the cellular elongation and differentiation[20,79]. As a future prospect, the integration of bioprinting technologies including 3D cell printing[80,81] to the porous nanosheets should provide more customized, tailor-made

tissue-engineered printed nanofilms by simple and instant manufacturing way.

3.6. Mussel-inspired polydopamine modified tissue-adhesive nanosheets for implantable devices

The development of implantable medical devices has made a tremendous contribution to the field of biomedical engineering[82]. These devices can monitor the physiological condition of the living body by interfacing with its interior surface[83,84] as well as intervening in functional body systems through the delivery of drugs[85,86] or physical energy like electricity[87,88] and light[13,14,36,89] to the target lesion. The standard choice for the fixation of implantable devices is surgical suturing; however, it is unsuitable for tissues near major nerves and blood vessels, as well as for fragile organs such as the brain, liver, and pancreas, that are mechanically fragile, actively deform, or move. Therefore, the development of ultra-conformable tissue-adhesive devices, which stick to living tissue surfaces like a sticker, is highly anticipated. Towards this goal, we focused on a mussel-foot-protein-inspired bio-adhesive polymer polydopamine (PDA) coating[57]. The surface of PDMS nanosheets were modified with PDA to develop tissue-adhesive PDA-PDMS nanosheets that allowed suture-free and long-term stable fixation of small implantable devices on wet internal living tissues[22]. The 650-nm-thick PDA-PDMS nanosheets with an elastic modulus of 14.9 ± 0.60 MPa and a flexural rigidity of ~4.5×10^{-4} nN m showed 25-fold-stronger adhesion (50.7 μJ/cm^2) to chicken muscle than a 0.8-mm-thick PDMS sheet with a flexural rigidity of > 10^5 nN m (2.2 μJ/cm^2) and successfully achieved the stable fixation of a small IC tag on the abdominal wall of rats for a month.

Taking advantage of the PDA-PDMS nanosheet, we developed a tissue-adhesive wirelessly powered optoelectronic device for fully implantable, metronomic (low-dose and long-term) photodynamic therapy (mPDT)[90] by embedding a near-field-communication (NFC)-based red or green LED chip (**Fig. 3G, left**). When subcutaneously implanted in the cancer model mice with intradermally transplanted tumors (**Fig. 3G, middle**), the device

consecutively irradiated the tumor for 10 days, leading to significant antitumor effects (**Fig. 3G, right**). This mPDT device emits light at approximately 1,000-fold-lower intensity than conventional phototherapy approaches, and thus does not involve the risk of overheating healthy tissues. This implantable and wirelessly powered mPDT system may offer a new path to the application of PDT, especially for deep cancers that are difficult to treat with standard methods. In the future, by the introduction of emerging printing technologies into the tissue-adhesive nanosheets, the whole structure of implantable/wearable devices can be a thin film type. For example, the light emitting part of the mPDT devices can be replaced by an organic electroluminescence device[91,37] that provides broader light irradiation and more conformably fits the surface of target tissues to treat widely diffused lesions. Moreover, antenna coils for wireless communication[92] or organic photovoltaics for self-powering the device[76] can be directly printed on the nanosheets by several printing techniques including inkjet printing, screen printing and transfer printing, to generate fully printed nanofilm electronics.

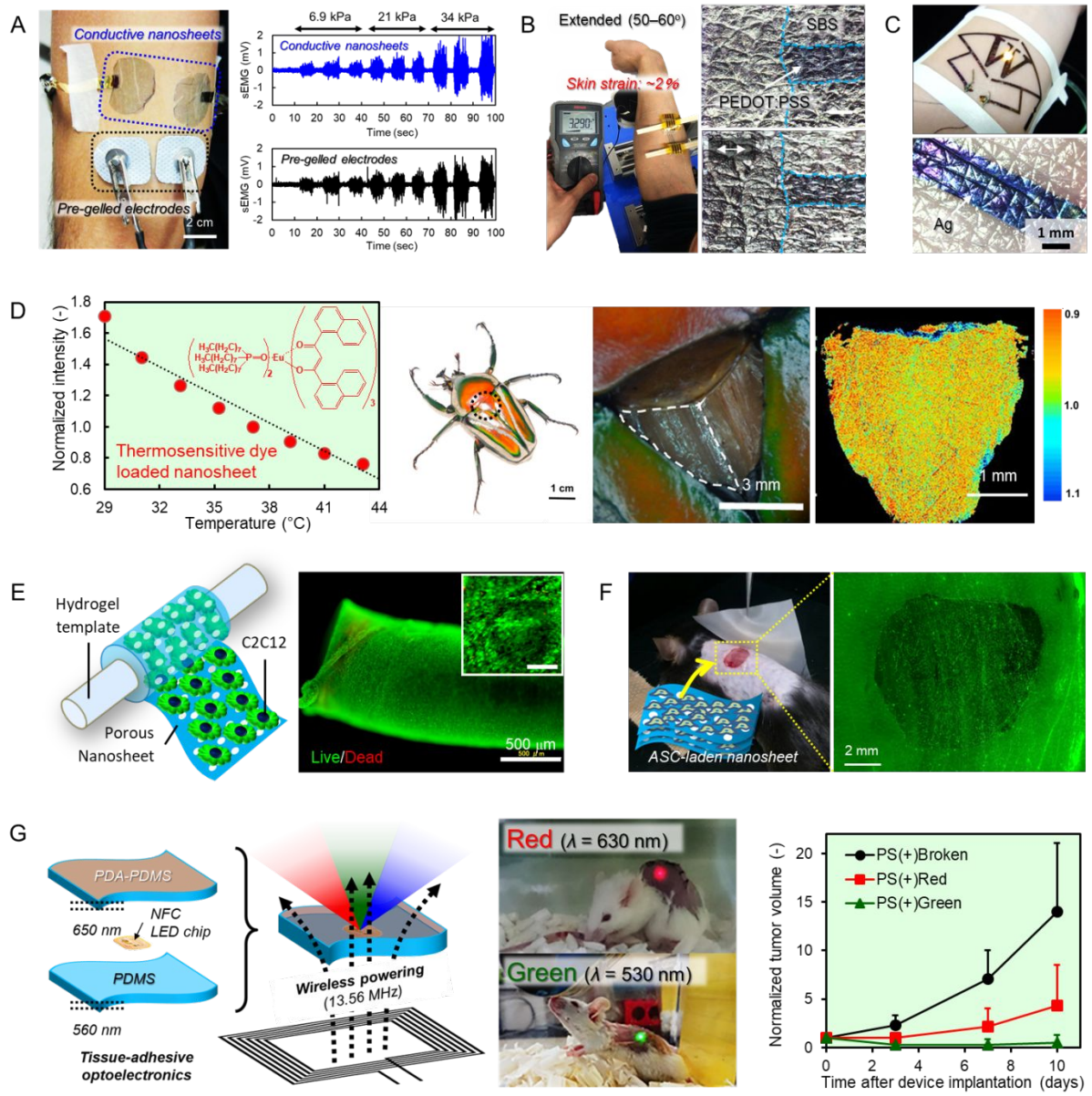

Fig. 3 Applications of printed nanofilms. (A) Image of conductive nanosheets and conventional pre-gelled electrodes adhered on the forearm of a subject (left) and the obtained sEMG signals (right) through them when the subject was grasping an analog pressure gauge at different levels of pressure. Reproduced from ref. 16. (B) Image of the measurement of the small skin strain using the nanosheet strain sensor attached to the forearm (left). The resistance of the sensor was measured when the wrist joint was extended and compared to that when not extended to calculate the skin strain. Microscopic images of the nanosheet strain sensor attached to a PDMS-based artificial skin model in the original (right, top) and stretched states (right, bottom). Scale bars represent 500 μm. Reproduced from ref. 17. (C) Image of

nanosheet electronics attached to the skin (top). An LED on an Ag-based circuit-printed SBS nanosheet is lit up on the skin. Microscopic image of the Ag line inkjet-printed on the SBS nanosheet adhered to skin (bottom). Reproduced from ref. 18. (D) Peak luminescence intensity of EuDT-laden nanosheet against different temperatures (left). The peak intensity was normalized by the value at 37°C. Image of *Dicronorrhina derbyana* beetle. The black dashed circle shows the location of a major flight muscle of the beetle (second from the left). Image of the nanosheet thermometer attached to the dorsal flight muscle of *D. derbyana*. The white dashed line shows the attached region of the nanosheet (second to the right). Temperature mapping of the dorsal flight muscle of *D. derbyana* during preflight preparation using stacked nanosheets (right). Reproduced from ref. 24. (E) Schematic illustration of a C2C12 cellular construct on a porous PDLLA nanosheet, rolled around a hydrogel-based tubular template (left). A live/dead fluorescent image of the rolled cellular construct with aligned myoblasts supported by the porous nanosheet (right). Inset: a magnified image (scale bar: 200 μm). Reproduced from ref. 28. (F) Image of the transference of a trilayered cell-laden porous nanosheet using nylon mesh to an incisional wound on a mouse (left). Fluorescent image of the trilayered cell-laden porous nanosheet attached on the incisional wound of the mouse (right). Reproduced from ref. 29. (G) Construction of the tissue-adhesive and wirelessly powered optoelectronic device composed of an NFC-based LED chip sandwiched between PDA–PDMS and pristine PDMS nanosheets (left). Images of red (middle, top) and green (middle, bottom) lighting emitted from wirelessly powered LED chips implanted subcutaneously in mice. The variation of the normalized tumor volume of the control [PS(+)broken] and two PDT groups [PS(+)red and PS(+)green] of mice. “PS(+)” means that the mice were injected with a photosensitizer (photofrin). “Broken” means that the implanted device had a disconnected circuit and hence did not emit any light. The tumor volumes measured on days 0, 3, 7, and 10 were divided by the initial volume for each tumor.

n = 10 for each group on each day. Reproduced from ref. 22.

4. Conclusions and outlook

We reviewed the seminal investigations of polymer nanosheets, namely, free-standing ultra-thin polymeric films, based on a variety of polymers and the development of printed nanofilms interfacing with the living body. The mechanical and adhesive properties of the polymer nanosheets, that are derived from their ultra-thin structure (< 1 μm) as well as their low flexural rigidity (< 10^{-2} nN m), not only provide conformal and stable physical adhesion to living tissue surfaces without suture or any adhesive agents but also solve the mechanical mismatch between relatively stiff materials and soft biological tissues. This unique property implies that the polymer nanosheets are promising as a mechanically compatible platform of wearable/implantable devices interfacing with the living body. Several examples of applications of printed nanofilms demonstrated that a variety of "inks" can be printed on polymer nanosheets and provide an unlimited range of applications. In the future, it is interesting and valuable to generate novel printed nanofilms with a range of functions by printing wide variety of inks or devices on polymer nanosheets, for example, chemical indicators, e.g. pH-, potential-, and gas-sensitive dyes; for environmental mapping, organic electronics including transistors, electroluminescent diodes, photovoltaics, and radical polymer batteries; for flexible electronics, microfluidics for health monitoring devices, antennas for wireless communication, and polymers, proteins and cells for tissue engineering . We believe that printed nanofilms will contribute to the progress of wearable/implantable devices in the regard of future medicine and healthcare as mechanically compatible nano-biointerfaces.

Acknowledgements

This work was supported by the Precursory Research for Embryonic Science and Technology

(PRESTO) from the Japan Science and Technology Agency (JST; grant number JPMJPR152A), and JSPS KAKENHI (grant number 17K20116, 18H03539, 18H05469), the Noguchi Institute, and the Tanaka Memorial Foundation.

Conflicts of interest

There are no conflicts of interest to declare.

References

1 Y. Liu, M. Pharr and G. A. Salvatore, *ACS Nano*, 2017, **11**, 9614–9635.

2 D.-H. Kim, N. Lu, R. Ma, Y.-S. Kim, R.-H. Kim, S. Wang, J. Wu, S. M. Won, H. Tao, A. Islam, K. J. Yu, T.-I. Kim, R. Chowdhury, M. Ying, L. Xu, M. Li, H.-J. Chung, H. Keum, M. McCormick, P. Liu, Y.-W. Zhang, F. G. Omenetto, Y. Huang, T. Coleman and J. A. Rogers, *Science*, 2011, **333**, 838–844.

3 B. Xu, A. Akhtar, Y. Liu, H. Chen, W. Yeo, S. I. I. Park, B. Boyce, H. Kim, J. Yu, H. Lai, S. Jung, Y. Zhou, J. Kim, S. Cho, Y. Huang, T. Bretl and J. A. Rogers, *Adv. Mater.*, 2016, **28**, 4462–4471.

4 S. Xu, Y. Zhang, L. Jia, K. E. Mathewson, K.-I. Jang, J. Kim, H. Fu, X. Huang, P. Chava, R. Wang, S. Bhole, L. Wang, Y. J. Na, Y. Guan, M. Flavin, Z. Han, Y. Huang and J. a Rogers, *Science*, 2014, **344**, 70–74.

5 D. Son, J. Lee, S. Qiao, R. Ghaffari, J. Kim, J. E. Lee, C. Song, S. J. Kim, D. J. Lee, S. W. Jun, S. Yang, M. Park, J. Shin, K. Do, M. Lee, K. Kang, C. S. Hwang, N. Lu, T. Hyeon and D.-H. Kim, *Nat. Nanotechnol.*, 2014, **9**, 397–404.

6 J. Jeong, W. Yeo, A. Akhtar, J. J. S. Norton, Y. Kwack, S. Li, S. Jung, Y. Su, W. Lee, J. Xia, H. Cheng, Y. Huang, W. Choi, T. Bretl and J. A. Rogers, *Adv. Mater.*, 2013, **25**, 6839–6846.

7 S. M. Lee, H. J. Byeon, J. H. Lee, D. H. Baek, K. H. Lee, J. S. Hong and S. Lee, *Sci.*

Rep., 2014, **4**, 6074.

8 C. Pang, C. Lee and K. Y. Suh, *J. Appl. Polym. Sci.*, 2013, **130**, 1429–1441.

9 X. Huang, Y. Liu, H. Cheng, W. Shin, J. A. Fan, Z. Liu, C. Lu, G. Kong, K. Chen, D. Patnaik, S. Lee, S. Hage-ali, Y. Huang and J. A. Rogers, *Adv. Funct. Mater.*, 2014, **24**, 3846–3854.

10 T. Yamada, Y. Hayamizu, Y. Yamamoto, Y. Yomogida, A. Izadi-Najafabadi, D. N. Futaba and K. Hata, *Nat. Nanotechnol.*, 2011, **6**, 296–301.

11 G. Lim, N. Lee and B. Lim, *J. Mater. Chem. C*, 2016, **4**, 5642–5647.

12 K. L. Montgomery, A. J. Yeh, J. S. Ho, V. Tsao, S. M. Iyer, L. Grosenick, E. A. Ferenczi, Y. Tanabe, K. Deisseroth, S. L. Delp and A. S. Y. Poon, *Nat. Methods*, 2015, **12**, 969–974.

13 G. Shin, A. M. Gomez, R. Al-Hasani, Y. R. Jeong, J. Kim, Z. Xie, A. Banks, S. M. Lee, S. Y. Han, C. J. Yoo, J. L. Lee, S. H. Lee, J. Kurniawan, J. Tureb, Z. Guo, J. Yoon, S. Il Park, S. Y. Bang, Y. Nam, M. C. Walicki, V. K. Samineni, A. D. Mickle, K. Lee, S. Y. Heo, J. G. McCall, T. Pan, L. Wang, X. Feng, T. il Kim, J. K. Kim, Y. Li, Y. Huang, R. W. Gereau, J. S. Ha, M. R. Bruchas and J. A. Rogers, *Neuron*, 2017, **93**, 509–521.

14 S. Il Park, D. S. Brenner, G. Shin, C. D. Morgan, B. A. Copits, H. U. Chung, M. Y. Pullen, K. N. Noh, S. Davidson, S. J. Oh, J. Yoon, K. Jang, V. K. Samineni, M. Norman, J. G. Grajales-reyes, S. K. Vogt, S. S. Sundaram, K. M. Wilson, J. S. Ha, R. Xu, T. Pan, T. Kim, Y. Huang, M. C. Montana, J. P. Golden, M. R. Bruchas, R. W. G. Iv and J. A. Rogers, *Nat. Biotechnol.*, 2015, **33**, 1280–1286.

15 T. Fujie, *Polym. J.*, 2016, **48**, 773–780.

16 A. Zucca, K. Yamagishi, T. Fujie, S. Takeoka, V. Mattoli and F. Greco, *J. Mater. Chem. C*, 2015, **3**, 6539–6548.

17 Y. Tetsu, K. Yamagishi, A. Kato, Y. Matsumoto, M. Tsukune, Y. Kobayashi, M. G.

Fujie, S. Takeoka and T. Fujie, *Appl. Phys. Express*, 2017, **10**, 087201.

18 M. Okamoto, M. Kurotobi, S. Takeoka, J. Sugano, E. Iwase, H. Iwata and T. Fujie, *J. Mater. Chem. C*, 2017, **5**, 1321–1327.

19 T. Fujie, Y. Mori, S. Ito, M. Nishizawa, H. Bae, N. Nagai, H. Onami, T. Abe, A. Khademhosseini and H. Kaji, *Adv. Mater.*, 2014, **26**, 1699–1705.

20 T. Fujie, S. Ahadian, H. Liu, H. Chang, S. Ostrovidof, H. Wu, H. Bae, K. Nakajima, H. Kaji and A. Khademhosseini, *Nano Lett.*, 2013, **13**, 3185–3192.

21 T. Fujie, H. Haniuda and S. Takeoka, *J. Mater. Chem.*, 2011, **21**, 9112.

22 K. Yamagishi, I. Kirino, I. Takahashi, H. Amano, S. Takeoka, Y. Morimoto and T. Fujie, *Nat. Biomed. Eng.*, 2018, DOI:10.1038/s41551-018-0261-7.

23 K. Yamagishi, S. Taccola, S. Takeoka, T. Fujie, V. Mattoli and F. Greco, in *Flexible and Stretchable Medical Devices*, ed. K. Takei, Wiley-VCH Verlag GmbH & Co. KGaA, Weinheim, 2018, pp. 253–283.

24 T. Miyagawa, T. Fujie, T. Thang, V. Doan, H. Sato and S. Takeoka, *ACS Appl. Mater. Interfaces*, 2016, **8**, 33377–33385.

25 T. Fujie, N. Matsutani, M. Kinoshita, Y. Okamura, A. Saito and S. Takeoka, *Adv. Funct. Mater.*, 2009, **19**, 2560–2568.

26 T. Fujie, A. Saito, M. Kinoshita, H. Miyazaki, S. Ohtsubo, D. Saitoh and S. Takeoka, *Biomaterials*, 2010, **31**, 6269–6278.

27 K. Ito, A. Saito, T. Fujie, K. Nishiwaki and H. Miyazaki, *Acta Biomater.*, 2015, **24**, 87–95.

28 S. Suzuki, K. Nishiwaki, S. Takeoka and T. Fujie, *Adv. Mater. Technol.*, 2016, **1**, 1600064.

29 K. Nishiwaki, S. Aoki, M. Kinoshita and T. Kiyosawa, *J. Biomed. Mater. Res. B*, 2018, DOI:10.1002/jbm.b.34228.

30 N. Kokubo, M. Arake, K. Yamagishi, Y. Morimoto, S. Takeoka, H. Ohta and T. Fujie, *ACS Appl. Bio Mater.*, 2018, DOI:10.1021/acsabm.8b00574.

31 D. Someya, S. Arai, T. Fujie and S. Takeoka, *RSC Adv.*, 2018, **8**, 35651–35657.

32 W.-C. Huang, H. Wu and C. J. Bettinger, *SPIE Newsroom*, 2016, DOI:10.1117/2.1201610.006638.

33 A. Tay, *MRS Bull.*, 2018, **43**, 566–567.

34 G. Hong, X. Yang, T. Zhou and C. M. Lieber, *Curr. Opin. Neurobiol.*, 2018, **50**, 33–41.

35 W. J. Tyler, *Nat. Rev. Neurosci.*, 2012, **13**, 867–878.

36 V. K. Samineni, J. Yoon, K. E. Crawford, Y. Ra, K. C. Mckenzie and G. Shin, *Pain*, 2017, **158**, 2108–2116.

37 T. Yokota, P. Zalar, M. Kaltenbrunner, H. Jinno, N. Matsuhisa, H. Kitanosako, Y. Tachibana, W. Yukita, M. Koizumi and T. Someya, *Sci. Adv.*, 2016, **2**, e1501856.

38 M. N. Hamdan, *Int. J. Mod. Nonlinear Theory Appl.*, 2012, **01**, 55–66.

39 B. Y. Okamura, K. Kabata, M. Kinoshita, D. Saitoh and S. Takeoka, *Adv. Mater.*, 2009, **21**, 4388–4392.

40 T. Fujie, Y. Kawamoto, H. Haniuda, A. Saito, K. Kabata, Y. Honda, E. Ohmori, T. Asahi and S. Takeoka, *Macromolecules*, 2013, **46**, 395–402.

41 F. Schneider, T. Fellner, J. Wilde and U. Wallrabe, *J. Micromechanics Microengineering Mech.*, 2008, **18**, 065008.

42 I. D. Johnston, *J. Micromechanics Microengineering*, 2014, **24**, 035017.

43 T. Fujie and S. Takeoka, in *Nanobiotechnology*, eds. D. A. Phoenix and A. Waqar, One Central Press, Altrincham, 2014, pp. 68–94.

44 T. Fujie, Y. Okamura and S. Takeoka, *Adv. Mater.*, 2007, **19**, 3549–3553.

45 N. Sato, A. Murata and S. Takeoka, *Soft Matter*, 2016, **12**, 9202–9209.

46 H. Watanabe, T. Ohzono and T. Kunitake, *Macromolecules*, 2007, **40**, 1369–1371.

47 C. M. Stafford, C. Harrison, K. L. Beers, A. Karim, E. J. Amis, M. R. VanLandingham, H.-C. Kim, W. Volksen, R. D. Miller and E. E. Simonyi, *Nat. Mater.*, 2004, **3**, 545–550.

48 S. Baba, T. Midorikawa and T. Nakano, *Appl. Surf. Sci.*, 1999, **144**–**145**, 344–349.

49 J. Sugano, T. Fujie, H. Iwata and E. Iwase, *Jpn. J. Appl. Phys.*, 2018, **57**, 06HJ04.

50 P. Bajaj, R. M. Schweller, A. Khademhosseini, J. L. West and R. Bashir, *Annu. Rev. Biomed. Eng.*, 2014, **16**, 247–276.

51 H. Cui, S. Miao, T. Esworthy, X. Zhou, S. jun Lee, C. Liu, Z. xi Yu, J. P. Fisher, M. Mohiuddin and L. G. Zhang, *Adv. Drug Deliv. Rev.*, 2018, **132**, 252–269.

52 Y. Li, Y. S. Zhang, A. Akpek, S. R. Shin and A. Khademhosseini, *Biofabrication*, 2017, **9**, 012001.

53 N. Ashammakhi, S. Ahadian, F. Zengjie, K. Suthiwanich, F. Lorestani, G. Orive, S. Ostrovidov and A. Khademhosseini, *Biotechnol. J.*, 2018, DOI:10.1002/biot.201800148.

54 E. Bihar, T. Roberts, Y. Zhang, E. Ismailova, T. Hervé, G. G. Malliaras, J. B. De Graaf, S. Inal and M. Saadaoui, *Flex. Print. Electron*, 2018, **3**, 34004.

55 E. Bihar, S. Wustoni, A. M. Pappa, K. N. Salama, D. Baran and S. Inal, *npj Flex. Electron.*, 2018, **2**, 30.

56 B. Nagar, M. Balsells, A. de la Escosura-Muñiz, P. Gomez-Romero and A. Merkoçi, *Biosens. Bioelectron.*, 2018, DOI:10.1016/j.bios.2018.09.073.

57 H. Lee, S. M. Dellatore, W. M. Miller and P. B. Messersmith, *Science*, 2007, **318**, 426–430.

58 A. Zucca, C. Cipriani, S. Tarantino, D. Ricci, V. Mattoli and F. Greco, *Adv. Healthc. Mater.*, 2015, **4**, 983–990.

59 S. H. Eom, S. Senthilarasu, P. Uthirakumar, S. C. Yoon, J. Lim, C. Lee, H. S. Lim, J. Lee and S. H. Lee, *Org. Electron. physics, Mater. Appl.*, 2009, **10**, 536–542.

60 B. Huber, J. Schober, A. Kreuzer, M. Kaiser, A. Ruediger and C. Schindler, *Microelectron. Eng.*, 2018, **194**, 85–88.

61 Z. Xiong and C. Liu, *Org. Electron. physics, Mater. Appl.*, 2012, **13**, 1532–1540.

62 L. M. Ferrari, S. Sudha, S. Tarantino, R. Esposti, F. Bolzoni, P. Cavallari, C. Cipriani, V. Mattoli and F. Greco, *Adv. Sci.*, 2018, **5**, 1700771.

63 A. Singh, M. Katiyar and A. Garg, *RSC Adv.*, 2015, **5**, 78677–78685.

64 S. K. Sinha, Y. Noh, N. Reljin, G. M. Treich, S. Hajeb-Mohammadalipour, Y. Guo, K. H. Chon and G. A. Sotzing, *ACS Appl. Mater. Interfaces*, 2017, **9**, 37524–37528.

65 X. He, R. He, Q. Lan, W. Wu, F. Duan, J. Xiao, M. Zhang, Q. Zeng, J. Wu and J. Liu, *Materials*, 2017, **10**, 220.

66 G. Istamboulie, T. Sikora, E. Jubete, E. Ochoteco, J. L. Marty and T. Noguer, *Talanta*, 2010, **82**, 957–961.

67 J. Griffin, A. J. Ryan and D. G. Lidzey, *Org. Electron. physics, Mater. Appl.*, 2017, **41**, 245–250.

68 N. Kumar, R. T. Ginting, M. Ovhal and J. W. Kang, *Mol. Cryst. Liq. Cryst.*, 2018, **660**, 135–142.

69 N. Chaturvedi and V. Dutta, *Energy Procedia*, 2013, **33**, 228–232.

70 K. Bock, *Proc. IEEE*, 2005, **93**, 1400–1406.

71 A. G. Kelly, D. Finn, A. Harvey, T. Hallam and J. N. Coleman, *Appl. Phys. Lett.*, 2016, **109**, 023107.

72 J. Barsotti, I. Hirata, F. Pignatelli, M. Caironi, F. Greco and V. Mattoli, *Adv. Electron. Mater.*, 2018, **4**, 1800215.

73 K. Fukuda, T. Sekine, R. Shiwaku, T. Morimoto, D. Kumaki and S. Tokito, *Sci. Rep.*,

2016, **6**, 27450.

74 K. Fukuda, Y. Takeda, Y. Yoshimura, R. Shiwaku, L. T. Tran, T. Sekine, M. Mizukami, D. Kumaki and S. Tokito, *Nat. Commun.*, 2014, **5**, 4147.

75 G. E. Bonacchini, C. Bossio, F. Greco, V. Mattoli, Y. H. Kim, G. Lanzani and M. Caironi, *Adv. Mater.*, 2018, **30**, 170691.

76 S. Park, S. W. Heo, W. Lee, D. Inoue, Z. Jiang, K. Yu, H. Jinno, D. Hashizume, M. Sekino, T. Yokota, K. Fukuda, K. Tajima and T. Someya, *Nature*, 2018, **561**, 516–521.

77 N. Piva, F. Greco, M. Garbugli, A. Iacchetti, V. Mattoli and M. Caironi, *Adv. Electron. Mater.*, 2017, **4**, 1700325.

78 A. Moya, G. Gabriel, R. Villa and F. Javier del Campo, *Curr. Opin. Electrochem.*, 2017, **3**, 29–39.

79 T. Fujie, A. Desii, L. Ventrelli, B. Mazzolai and V. Mattoli, *Biomed. Microdevices*, 2012, **14**, 1069–1076.

80 H. Lee, Y. Koo, M. Yeo, S. Kim and G. H. Kim, *Int. J. Bioprinting*, 2017, **3**, 27–4.

81 J. Jang, J. Y. Park, G. Gao and D. W. Cho, *Biomaterials*, 2018, **156**, 88–106.

82 Y.-H. Joung, *Int. Neurourol. J.*, 2013, **17**, 98–106.

83 T.-M. Fu, G. Hong, T. Zhou, T. G. Schuhmann, R. D. Viveros and C. M. Lieber, *Nat. Methods*, 2016, **13**, 875–882.

84 C. Baj-Rossi, A. Cavallini, E. G. Kilinc, F. Stradolini, T. R. Jost, M. Proietti, G. De Micheli, F. Grassi, C. Dehollain and S. Carrara, *IEEE Trans. Biomed. Circuits Syst.*, 2016, **10**, 955–962.

85 I. R. Minev, P. Musienko, A. Hirsch, Q. Barraud, N. Wenger, E. M. Moraud, J. Gandar, M. Capogrosso, T. Milekovic, L. Asboth, R. F. Torres, N. Vachicouras, Q. Liu, N. Pavlova, S. Duis, A. Larmagnac, J. Vörös, S. Micera, Z. Suo, G. Courtine and S. P. Lacour, *Science*, 2015, **347**, 159–163.

86 A. Jonsson, Z. Song, D. Nilsson, B. A. Meyerson, D. T. Simon, B. Linderoth and M. Berggren, *Sci. Adv.*, 2015, **1**, e1500039.

87 D. Reynolds, G. Z. Duray, R. Omar, K. Soejima, P. Neuzil, S. Zhang, C. Narasimhan, C. Steinwender, J. Brugada, M. Lloyd, P. R. Roberts, V. Sagi, J. Hummel, M. G. Bongiorni, R. E. Knops, C. R. Ellis, C. C. Gornick, M. A. Bernabei, V. Laager, K. Stromberg, E. R. Williams, J. H. Hudnall and P. Ritter, *N. Engl. J. Med.*, 2016, **374**, 533–541.

88 D. R. Agrawal, Y. Tanabe, D. Weng, A. Ma, S. Hsu, S. Liao, Z. Zhen, Z. Zhu, C. Sun, Z. Dong, F. Yang, H. F. Tse, A. S. Y. Poon and J. S. Ho, *Nat. Biomed. Eng.*, 2017, **1**, 0043.

89 J. Jeong, J. G. Mccall, G. Shin, Y. Huang, M. R. Bruchas, J. A. Rogers, J. Jeong, J. G. Mccall, G. Shin, Y. Zhang, R. Al-hasani, M. Kim and S. Li, *Cell*, 2015, **162**, 1–13.

90 S. K. Bisland, L. Lilge, A. Lin, R. Rusnov, B. C. Wilson, S. K. Bisland, L. Lilge, A. Lin, R. Rusnov and B. C. Wilson, *Photochem. Photobiol.*, 2004, **80**, 22–30.

91 J. R. Sheats, H. Antoniadis, M. Hueschen, W. Leonard, J. Miller, R. Moon, D. Roitman and A. Stocking, *Science*, 1996, **273**, 884–888.

92 M. S. Mannoor, H. Tao, J. D. Clayton, A. Sengupta, D. L. Kaplan, R. R. Naik, N. Verma, F. G. Omenetto and M. C. McAlpine, *Nat. Commun.*, 2012, **3**, 763.

Author Introduction:

Kento Yamagishi

Kento Yamagishi, Ph.D., is a Research Fellow in Digital Manufacturing and Design (DManD) Center at Singapore University of Technology and Design (SUTD) and a visiting researcher in Research Organization for Nano & Life Innovation at Waseda University (concurrently). He received his Ph.D. in Engineering from Waseda University in 2018, where he held a Fellowship of Japan Society for Promotion of Science. He spent a postdoctoral period in Research Organization for Nano & Life Innovation at Waseda University (2018) and moved to the DManD Center at SUTD in 2018. His research interests are dedicated for the development of biomaterials and biomedical devices for wearable/implantable applications. His honors include the Young Scientist Presentation Award from the Japan Society of Applied Physics (JSAP), Japan (2015).

Shinji Takeoka

Shinji Takeoka, Ph.D., is a Professor in the Faculty of Science and Engineering at Waseda University. He received his Ph.D. in Engineering from Waseda University in 1991, where he held a Fellowship of Japan Society for Promotion of Science. He worked as a visiting researcher at University of Pennsylvania (1999) and became a Professor in the Faculty of Science and Engineering at Waseda University in 2007. He is concurrently a Professor in Cooperative Major in Advanced Biomedical Sciences, Joint graduate school of Tokyo Women's Medical University and Waseda University since 2010. His research interests are dedicated for molecular assembling science and engineering in order to design and construct the nanomaterials in biomedical applications. His honors include the Okuma Memorial Academic Prize, Waseda University (2011).

Toshinori Fujie

Toshinori Fujie, Ph.D., is an Associate Professor in the Waseda Institute for Advanced Study (WIAS) at Waseda University, and an Associate Professor (Lecturer) in the School of Life Science and Technology at the Tokyo Institute of Technology. He received his Ph.D. in Engineering from Waseda University in 2009. He spent postdoctoral periods at the Italian Institute of Technology (2010–2012) and Tohoku University (2012–2013), and joined as an Assistant Professor of the Faculty of Science and Engineering at Waseda University in 2013, and moved to the WIAS at Waseda University in 2016. He has concurrently served as a PRESTO researcher at the Japan Science and Technology Agency (JST) since 2015. His research interests are dedicated for biomaterials, tissue engineering and biorobotics in the application of advanced medicine and healthcare. His honors include The Award for Young Investigator of Japanese Society for Biomaterials (2017) by Japanese Society for Biomaterials, and the Young Scientists' Prize for the Commendation for Science and Technology by the Minister of Education, Culture, Sports, Science and Technology (MEXT), Japan (2018).